Nature and Science of Sleep

Dovepress
open access to scientific and medical research

Open Access Full Text Article

ORIGINAL RESEARCH

Characteristics and Mechanism of Upper Airway Collapse Revealed by Dynamic MRI During Natural Sleep in Patients with Severe Obstructive Sleep Apnea

Yuqi Li[1,2,*], Changjin Ji[1,2,*], Weiao Sun[1,2], Huahui Xiong[1,2], Zheng Li[3], Xiaoqing Huang[1,2], Tingting Fan[1,2], Junfang Xian[3], Yaqi Huang[1,2]

[1]School of Biomedical Engineering, Capital Medical University, Beijing, People's Republic of China; [2]Beijing Key Laboratory of Fundamental Research on Biomechanics in Clinical Application, Capital Medical University, Beijing, People's Republic of China; [3]Department of Radiology, Beijing Tongren Hospital, Capital Medical University, Beijing, People's Republic of China

*These authors contributed equally to this work

Correspondence: Yaqi Huang, School of Biomedical Engineering, Capital Medical University, Beijing, People's Republic of China, Tel +86-10-83911809, Email yqhuang@ccmu.edu.cn; Junfang Xian, Department of Radiology, Beijing Tongren Hospital, Capital Medical University, Beijing, People's Republic of China, Email cjr.xianjunfan@vip.163.com

Purpose: Upper airway collapse during sleep in patients with obstructive sleep apnea (OSA) is a complex and dynamic phenomenon. By observing and analyzing the dynamic changes in the upper airway and its surrounding tissues during airway obstruction, we aim to reveal dynamic characteristics in different obstruction patterns, and the relationship between anatomical features during normal breathing and dynamic characteristics of airway obstruction.

Patients and Methods: Dynamic MRI was performed in 23 male patients (age range 26–63) with severe OSA diagnosed by overnight polysomnography, and obstruction events were identified from their images. Dynamic changes in parameters of the upper airway and surrounding tissues were measured to assess the key characteristics in different obstruction patterns.

Results: We categorized airway obstruction into four types based on the obstruction location and motion characteristics of tissues during collapse, and detailed the alterations in the airway and surrounding tissues under each obstruction pattern. In all 112 obstruction events extracted from the dynamic images of 23 patients, type A (retropalatal obstruction caused by the soft palate separated from the tongue), BI, BII (both retropalatal obstructions caused by the soft palate attached to the tongue, and C (retropalatal and retroglossal obstruction caused by the soft palate and the tongue), accounted for 28.6%, 44.6%, 12.5%, and 14.3% respectively. In severe OSA patients with tongue and palatal obstruction related to type B or C, the more posterior hyoid position, shorter distance between tongue and uvula, and wider retropalatal space, the larger the tongue displacement and deformation during collapse, and the greater the reduction in airway space.

Conclusion: There are multiple airway obstruction patterns, each with its own anatomical characteristics and behaviors during collapse. Hyoid position, tongue and uvula distance, and retropalatal space play an important role in airway collapse and should be paid more attention in the treatment of OSA.

Keywords: airway obstruction patterns, obstruction location, tissue motion characteristics, hyoid position, retropalatal space

Introduction

Obstructive sleep apnea (OSA) is characterized by repetitive collapse of the upper airway during sleep, resulting in hypopnea or apnea.[1,2] The primary etiologies of OSA are thought to be linked to abnormal upper airway anatomy and reduced neural control of pharyngeal muscles,[3–6] leading to dynamic collapses of multiple patterns.[7–9] Surgical intervention is one of the main interventions for OSA. However, the selection of surgical approaches is influenced

Received: 28 May 2023
Accepted: 19 October 2023
Published: 1 November 2023

significantly by various clinical factors, such as the pattern of upper airway collapse and the patient's clinical status. Surgery's success largely depends upon the personal judgement of the doctor and the utilization of appropriate techniques.[10] Investigating the mechanism of upper airway collapse in OSA patients is of great clinical significance to understand the pathogenesis and select optimal treatments.

Magnetic resonance imaging (MRI) is commonly used to assess anatomical abnormalities in the upper airway or surrounding tissues in OSA patients.[11,12] MRI studies have shown that OSA patients are characterized by an oversized tongue and soft palate, narrowed cross-sectional areas of the airway, downshifted hyoid, and increased airway length compared to healthy individuals.[13–19] Although conventional MRI has significant advantage in identifying anatomical features in patients with OSA, its scan time is often much longer than the duration of the respiratory cycle or upper airway obstruction, and therefore it cannot capture the dynamic process of upper airway obstruction. The results obtained by MRI may vary widely when a particular tissue changes significantly during airway collapse. Therefore, conventional MRI has obvious limitations in studying the process of upper airway collapse during sleep.

Dynamic MRI, which capture a series of images in quick succession to create a movie-like sequence of tissue in motion,[20] can record the process of airway changes and tissue deformation during respiratory cycles or obstruction events.[21] Dynamic MRI studies in awake state show changes in airway morphology during breathing in OSA patients compared with healthy subjects, including increased airway compliance and reduced airway ellipticity.[22,23] Dynamic MRI studies during drug-induced or natural sleep can capture airway obstruction in OSA patients, such as retropalatal and retroglossal collapse, airway space changes, and tongue or soft palate movement. Upper airway obstruction can be classified according to the collapse site.[7,8] Most studies focus on the changes of the airway itself during breathing or collapse, but ignore the movement of its surrounding tissues.[24–26] Because the airway is a cavity enclosed by the head and neck tissues, and its collapse is caused by the movement of surrounding tissues, it is crucial to uncover tissue movement patterns during the collapse process to understand the mechanism behind airway collapse. Previous studies using dynamic MRI have also observed the dynamic changes in the tongue, soft palate, and uvula, showing that the range of tongue and soft palate movements during sleep was greater in OSA patients than in healthy individuals.[27,28] However, these studies have not analyzed the movements and morphological changes of tissues during airway collapse, which is of great significance for understanding the mechanism of different types of airway obstruction.

The present study aims to investigate the process of upper airway collapse during natural sleep in patients with severe OSA using dynamic MRI. We will analyze the characteristic changes of the upper airway and surrounding tissues under different obstruction patterns, compare the anatomical features during normal breathing in OSA patients with different obstruction patterns, and establish correlations between anatomical structural features and dynamic motion characteristics, which can lead to a better understanding of the mechanisms of airway obstruction and help in the development of personalized treatments for OSA.

Materials and Methods

Subjects and Dynamic MRI Examinations

All subjects are Asian males. Exclusion criteria include lung disease, upper airway tissue lesions, psychiatric disorders, and severe cardiovascular disease. None of them had received any surgical treatment for OSA prior to joining the study. All patients were monitored overnight using a noninvasive polysomnography (SOMNO HD, SOMNOmedics, Germany) under standard procedures. Apnea-hypopnea index (AHI) was confirmed by a professional sleep physician based on polysomnography data. Finally, 31 patients with severe OSA diagnosed with AHI >30 were enrolled for dynamic MRI scans during natural sleep.

The participants were asked to sleep less the night before so that they could fall asleep naturally during the MRI scan without the use of any sedatives. Each patient was supine with his heads in an 8-channel head and neck combination coil secured with sponge pads and earplugs in both ears. The nasal airflow was inputted into the sleep monitor (EMBLA N7000, Reykjavik, Iceland) via a nasal cannula. If the nasal airflow signal indicated repetitive pauses lasting more than 10 seconds, the subject was deemed asleep, and the dynamic MRI scan was initiated. Dynamic MRI scans were carried out with a fast gradient-echo sequence using a 3.0T MRI scanner (GE Healthcare, Milwaukee, Wisconsin, USA) on the

mid-sagittal plane of the head and neck. The scan parameters included TR/TE = 7.6/1.9 ms, a flip angle of 12°, a matrix of 256×256, and a layer thickness of 16 mm. The average scan time for each participant was 120 s. The total number of mid-sagittal images acquired was 128. Patients who exhibited excessive head movement during dynamic MRI or did not show upper airway obstruction were excluded. Ultimately, 23 male patients with severe OSA were included in the study. The protocol was approved by the Ethics Committee of Capital Medical University, Beijing, China (2013SY67). All subjects signed the informed consent prior to participation. This study was conducted in accordance with the Declaration of Helsinki.

Acquisition of Dynamic Parameters

We manually segmented structures frame-by-frame from the dynamic images. Figure 1A shows the tissues and airway extracted from the images, which include the tongue, soft palate, hyoid bone, retropalatal and retroglossal airway. Then, morphological parameters were measured, and the centers of the tongue, soft palate, and hyoid bone were calculated separately to characterize the position of each structure.

To make the results from different subjects comparable, the vertebral coordinate system was established based on the C3 and C4 vertebrae, as shown in Figure 1B, and the coordinates of all tissue centers were in the vertebral coordinate system. The morphological parameters of the tissues, including the long axis of the tongue (L_{LAX}), the short axis of the tongue (L_{SAX}), the hard palate-soft palate angle (α), the soft palate-tip of the uvula angle (β), and the soft palate length (L_{SP}), as shown in Figure 1B, were measured. The aspect ratio of the tongue, $AR_{Tg} = L_{LAX}/L_{SAX}$, was calculated. The upper airway parameters included the minimum width of the retropalatal space ($minW_{RP}$) and the minimum and mean width of the retroglossal space ($minW_{RG}$ and mW_{RG}). We also measured the distance between the tongue center and the tip of the uvula (L_{TgU}) to assess the relative position between the tongue and the uvula.

The stable values of the parameters during airway obstruction were measured at each obstruction event. The average values of the parameters in a time interval of approximately 4 seconds before obstruction were calculated as the baseline at the time of airway opening for this obstruction event. The change of a parameter due to the obstruction event was then obtained by subtracting the value of the obstruction state from the value of the opening state.

Classification of Upper Airway Obstruction Pattern

Based on dynamic MRI images of the mid-sagittal plane, we classified the types of airway obstruction according to the motion characteristics of the soft palate and tongue during collapse. We grouped the patients based on their obstruction

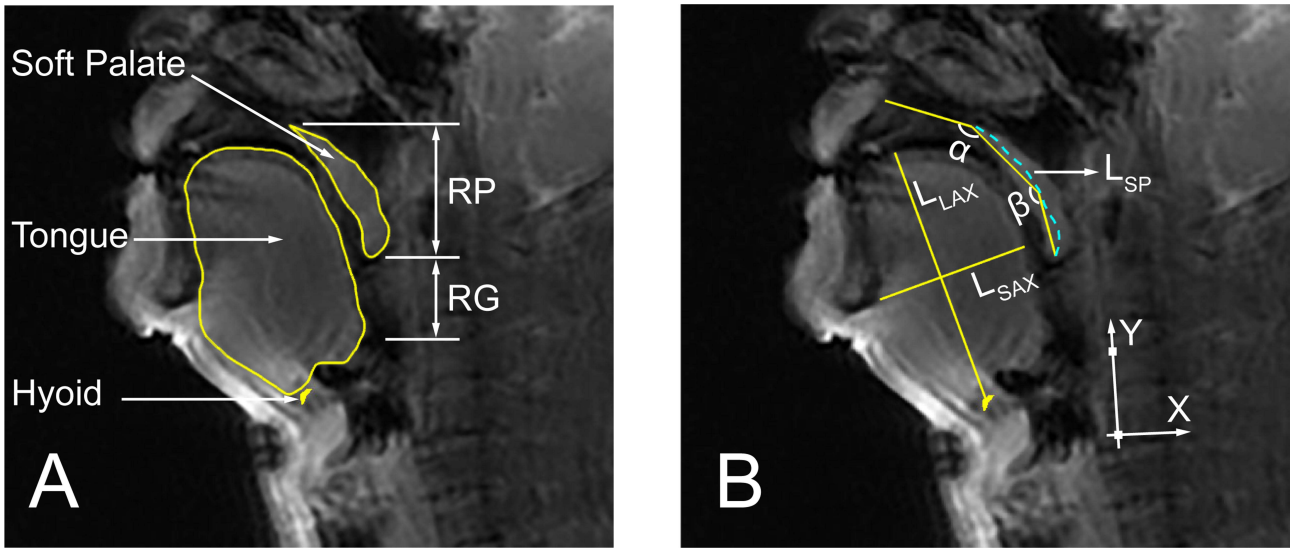

Figure 1 Schematic diagram of the tissues (**A**) and morphological parameters (**B**) to be extracted. RP: Retropalatal; RG: Retroglossal region; L_{LAX}: The long axis of the tongue; L_{SAX}: the short axis of the tongue; α: the angle between the hard palatal and the soft palate; β: the angle between the soft palate and the uvula; L_{SP}: The length of soft palate. Coordinate system is built by the front upper point of C3 and the front lower point of C4.

type for our statistical analysis. If a patient had multiple types of airway obstruction, the patient was classified based on the longest cumulative time for the type of obstruction. As well, we characterized the airway anatomical parameters in normal breathing status of the patients using the mean value of the parameters during airway opening.

Statistical Analysis

The data of all subjects were analyzed using SPSS software (SPSS Inc, Chicago, USA). Paired-sample nonparametric tests were conducted to compare various parameters in both the airway opening and collapse states. The independent sample nonparametric test was used to evaluate the parameter changes of different types of obstruction events and the anatomical parameters in normal breathing status of subjects with different types of obstruction. When p-values < 0.05, the difference was considered statistically significant. Spearman correlation analysis was used to test the correlations of anatomical parameters and parameter changes.

Results

A total of 112 obstruction events were extracted from the images of 23 patients. The basic characteristics of the patients were given in Table 1.

Upper Airway Obstruction Pattern

We first categorized airway obstruction into three major patterns based on dynamic MRI in the mid-sagittal plane, as shown in Figure 2. These patterns included retropalatal obstruction caused by a backward movement of the soft palate separated from the tongue (Type A), retropalatal obstruction due to a backward movement of the soft palate attached to the tongue (Type B), and retropalatal and retroglossal obstruction arising from a combined backward movement of the soft palate and the tongue (Type C).

However, there were two distinct tissue movement patterns within type B obstruction. This prompted us to further subdivide type B obstruction into type BI and type BII. Both subtypes were characterized by retropalatal obstructions resulted from tongue pushing against the soft palate, but they exhibited different tissue movements. Supplementary dynamic schematic diagrams of the four obstruction patterns are presented in the attached Video File, which can clearly distinguish between BI and BII obstruction.

Figure 3 shows the distribution of different airway obstruction patterns. Subfigures A and B are based on subjects and events, respectively. Of the 23 patients, 82.7% exhibited a single type of obstruction, and 17.3% showed multiple types of airway obstruction. More than half of the subjects presented with type B obstruction, much higher than the others. Notably, type BI obstruction event occurred most frequently, accounting for approximately 44.6% of all obstruction events.

During the MRI scan, 10 of the 23 people had oral breathing. Six of them were breathing orally at the time of the airway obstruction. Oral breathing had the greatest impact on type A, accounting for half of the obstruction events (16/32). In patients with BI and BII types, 16% (8/50) and 14% (2/14), respectively, had oral breathing at the time of obstruction, while no oral breathing occurred in type C patients.

Table 1 Basic Characteristics of 23 Asian Male Participants

	Mean± Standard Deviation	Range
Age, years	43.78 ± 9.74	26.00 to 63.00
BMI, $kg{\bullet}m^{-2}$	27.36 ± 4.06	21.60 to 38.90
AHI, times/h	56.48 ±15.10	31.20 to 84.30

Abbreviations: BMI, body mass index; AHI, apnea-hypopnea index.

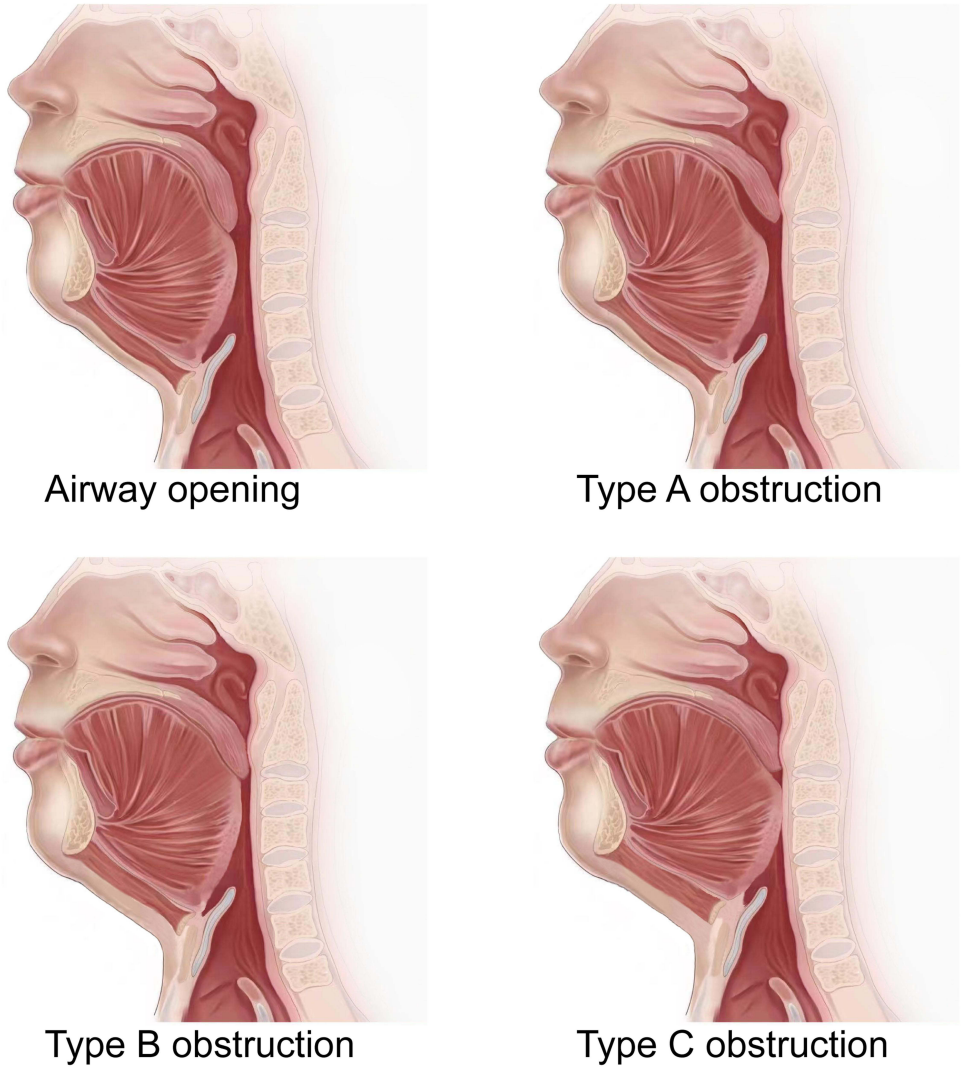

Figure 2 Schematic diagram of upper airway opening and different types of obstruction.

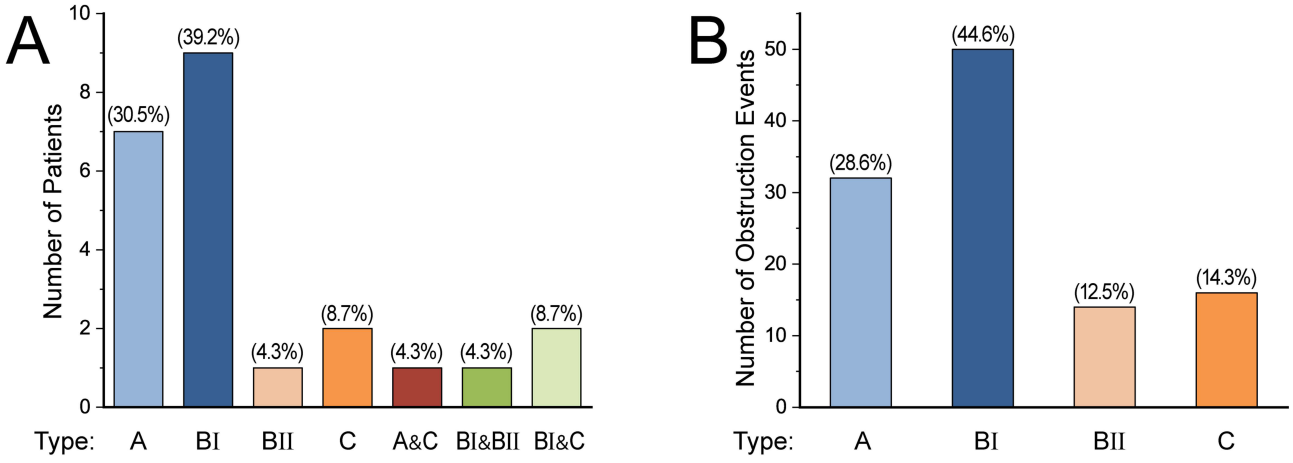

Figure 3 Distribution features of airway obstruction in 23 subjects (**A**) and in 112 obstruction events (**B**). The data in brackets at the top of each rectangular diagram is the percentage of a given obstruction type.

Dynamic Changes of Upper Airway Obstruction

Figure 4A and B show the displacement of the hyoid center in the X and Y directions, ΔX_{Ho} and ΔY_{Ho}, respectively, during airway obstruction. It could be seen that the hyoid remained stable during type A obstruction without significant

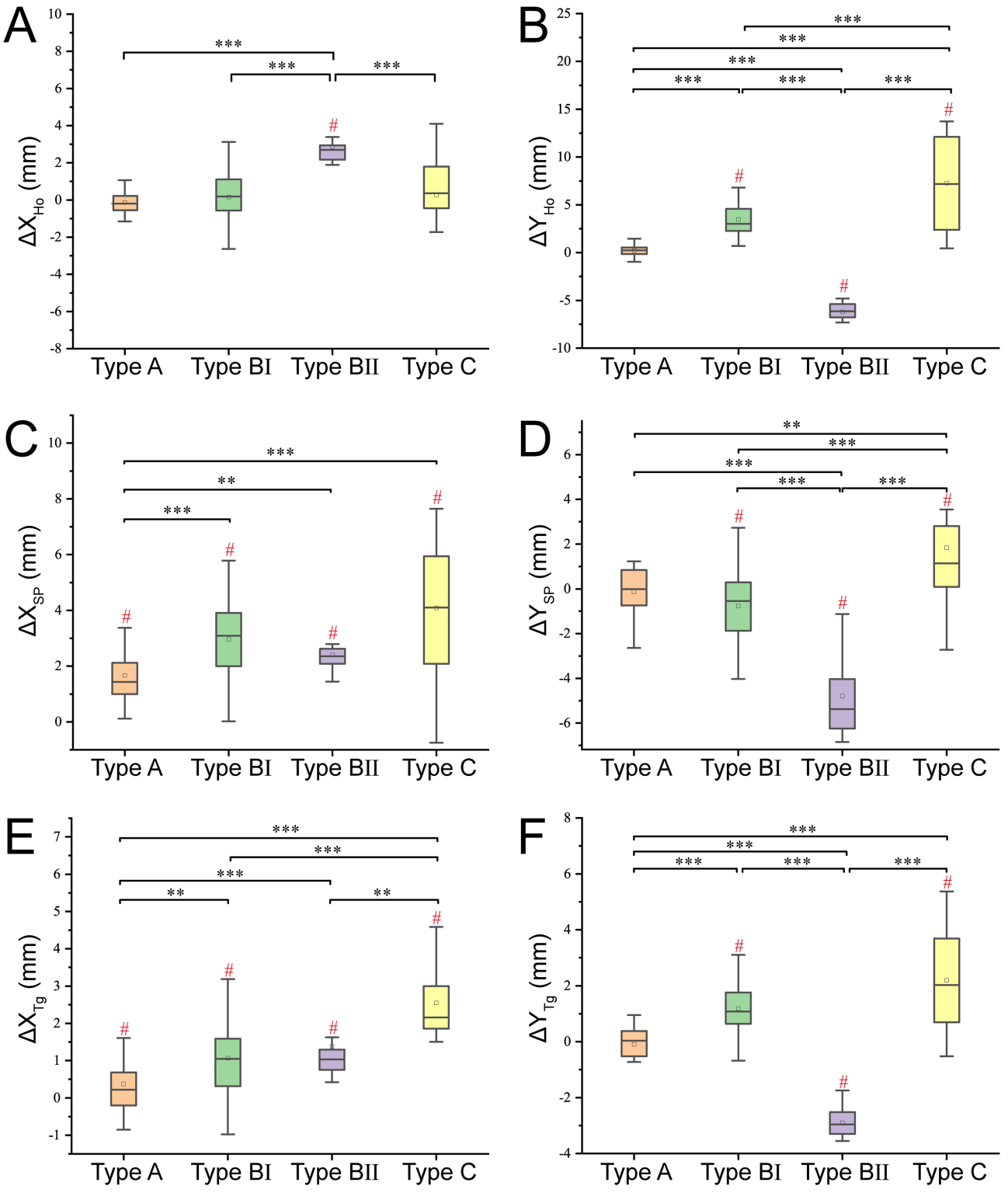

Figure 4 Dynamic characteristics of the displacement of each tissue centroid during airway obstruction of type A, BI, BII, and C. (**A** and **B**) ΔX_{Ho} and ΔY_{Ho}, displacement of the hyoid center in the X-direction and Y-direction. (**C** and **D**) ΔX_{SP} and ΔY_{SP}, displacement of the soft palate center in the X-direction and Y-direction. (**E** and **F**) ΔX_{Tg} and ΔY_{Tg}, displacement of the tongue center in the X-direction and Y-direction. The hash #Indicates that the change of the centroid location itself during airway obstruction is significant, p-value < 0.05. The asterisk indicates that the displacement with different types of obstruction is significantly different. **p-value <0.01, ***p-value <0.001.

displacement. However, the hyoid moved significantly upward in type BI, and downward and toward the posterior wall of the airway in type BII. The hyoid moved upward in type C, and the displacement was significantly larger than that in type BI.

Figure 4C and D show the displacement of the soft palate center in the X and Y directions, ΔX_{SP} and ΔY_{SP}, respectively, during airway obstruction. Although the soft palate moved toward the posterior airway wall in type A, its displacement was comparatively smaller than in the other three types of obstruction. The soft palate moved downward and toward the posterior airway wall in type BI, and the displacement trend in type BII was similar to that in type BI, with the exception of a greater downward displacement than that in type BI. The soft palate exhibited upward and posterior displacement in type C.

Figure 4E and F show the displacement of the tongue center in the X and Y directions, ΔX_{Tg} and ΔY_{Tg}, respectively, during airway obstruction. Type A obstruction resulted in a posterior displacement of the tongue, which was comparatively smaller than that in the other three types of obstruction. The tongue moved upward and toward the posterior airway wall in type BI. But the tongue moved downward and toward the posterior airway wall in type BII. The displacement trend of the tongue in type C was the same as that in type BI, except that the posterior displacement of the tongue was larger in type C obstruction.

Figure 5 shows the alterations in the morphological parameters of the tongue and soft palate during airway obstruction. As shown in Figure 5A, there was no significant change in the aspect ratio of the tongue, ΔAR_{Tg}, during type A obstruction. However, ΔAR_{Tg} in type BI exhibited an obvious decline, which was mainly due to the shortening of ΔL_{LAX} and the lengthening of ΔL_{SAX}, as shown in Figure 5B and C. By contrast, ΔAR_{Tg} exhibited a significant increase in type BII, which was primarily driven by a large increase in ΔL_{LAX}. The trend of ΔAR_{Tg} in type C was similar to that in type BI. The difference was that the ΔAR_{Tg} change in type C was greater. Figure 5D shows the change in the length of the soft palate, ΔL_{SP}, during airway obstruction. Notably, all four types of obstruction exhibited an elongation in ΔL_{SP}, with the least significant increase in type A and the most pronounced increase in type BII.

Figure 5E and F show the change in the angles of the hard palate-soft palate, $\Delta\alpha$, and soft palate-tip of the uvula, $\Delta\beta$, during airway obstruction. The angle $\Delta\alpha$ increased significantly during type A, BI and C obstruction, while it decreased significantly in type BII obstruction. For the angle $\Delta\beta$, there was no significant change in type A and BII obstruction, reflecting the constant curvature of the soft palate. However, $\Delta\beta$ decreased significantly in type BI and C obstruction, indicating increased curvature of the soft palate in response to airway obstruction.

Figure 6A and B show the percentage changes in the mean and minimum width of the retroglossal space, ΔmW_{RG} and $\Delta minW_{RG}$, during airway obstruction. Both ΔmW_{RG} and $\Delta minW_{RG}$ experienced significant reductions during all types of obstruction. Type A obstruction resulted in the lowest reduction in both width parameters of the retroglossal space. Types BI and BII resulted in greater reduction, whereas type C resulted in complete closure of the retroglossal space.

Anatomical Features

Table 2 shows the characteristics of the study participants, including age, BMI, AHI, and upper airway anatomical parameters measured during normal breathing. No significant differences were observed in age, BMI, and AHI in these patients. Among the 23 patients, 7 were dominated by type A obstruction, 9 by type BI obstruction, 2 by type BII obstruction, and 5 by type C obstruction. The differences of X_{Ho}, L_{TgU}, $minW_{RP}$, and mW_{RG} among the patients were statistically significant.

During normal breathing, patients with type A dominated obstruction exhibited larger L_{TgU} and $|X_{Ho}|$, which can be used to estimate roughly the distance from the hyoid to the posterior wall of the airway, and smaller $minW_{RP}$ compared with other patients, indicating that in patients with type A dominated obstruction the hyoid was more anteriorly positioned, the distance between the tongue and uvula was longer, and the retropalatal space was smaller. The value of mW_{RG} was larger in patients with type BI dominated obstruction, suggesting a larger retropalatal space compared to other patients, especially patients with type C dominated obstruction. No significant anatomical features were identified in patients with type BII dominated obstruction, possibly due to the relatively smaller number of patients in this group. Patients with type C dominated obstruction displayed a significantly larger retropalatal space, smaller retroglossal space,

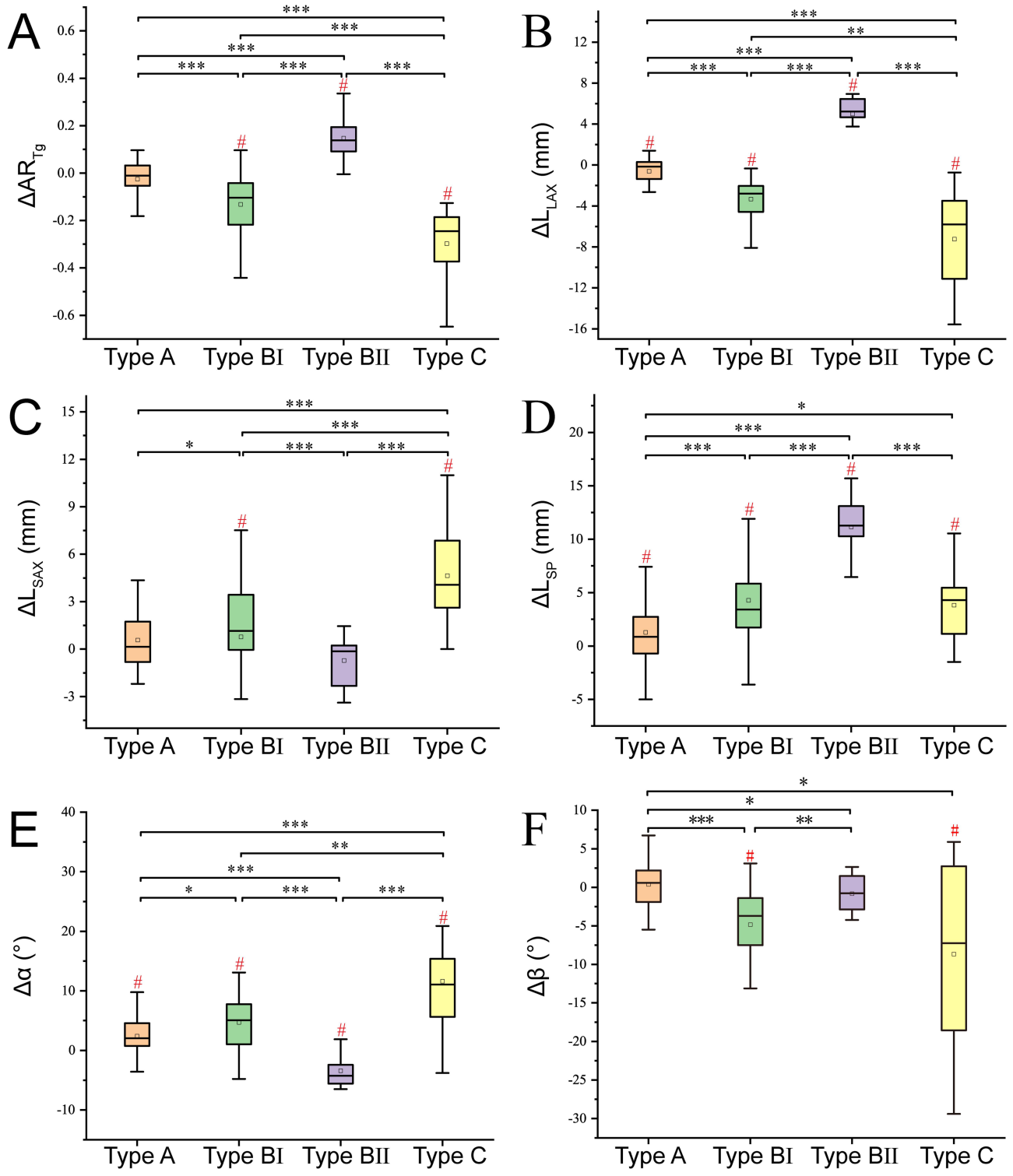

Figure 5 Dynamic characteristics of tongue and soft palate morphology changes during airway obstruction. (**A**) ΔAR_{Tg}, variation of the aspect ratio of the tongue. (**B**) ΔL_{LAX}, variation of the long axis of the tongue. (**C**) ΔL_{SAX}, variation of the short axis of the tongue. (**D**) ΔL_{SP} variation of the length of soft palate. (**E**) $\Delta\alpha$, variation of the angle between the hard and soft palate. (**F**) $\Delta\beta$, variation of the angle between the soft palate and uvula. The hash #Indicates that the change of the centroid location itself during airway obstruction is significant, p-value <0.05. The asterisk *Indicates that the displacement with different types of obstruction is significantly different. *p-value < 0.05, **p-value <0.01, ***p-value <0.001.

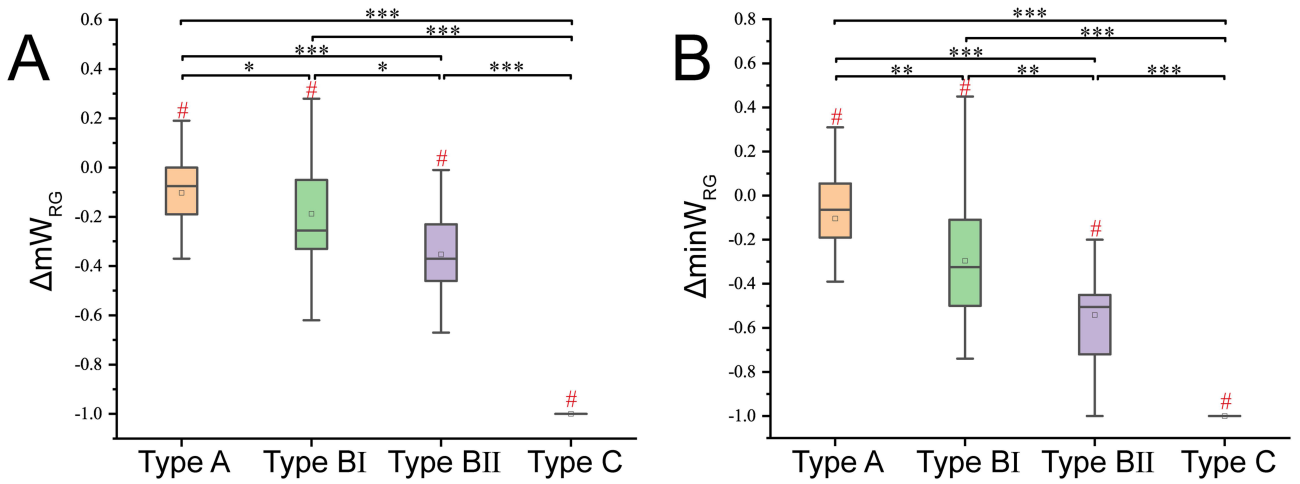

Figure 6 Dynamic characteristics of the mean width ΔmW_{RG} (**A**) and the minimum width $\Delta minW_{RG}$ (**B**) of the retroglossal space changes during airway obstruction. The hash #Indicates that the change of the centroid location itself during airway obstruction is significant, p-value <0.05. The asterisk *Indicates that the displacement with different types of obstruction is significantly different. *p-value <0.05, **p-value <0.01, ***p-value <0.001.

and smaller distance between the hyoid and the posterior airway wall compared with patients with type A dominated obstruction.

Correlation of Anatomical Features and Dynamic Changes

Figure 7 shows the heat map of correlation analysis between the anatomical features in normal breathing and dynamic changes during airway obstruction. The results show that, among the anatomical features, the X-direction position of the hyoid, X_{Ho}, the distance between the tongue center and the tip of the uvula, L_{TgU}, and the minimum width of the retropalatal space, $minW_{RP}$, were significantly correlated with many dynamic changes during airway obstruction. These correlations highlight the important influence of these anatomical features on the process of upper airway obstruction.

As shown in Figure 8A–F, X_{Ho} was positively correlated with $\Delta\alpha$, ΔX_{Tg}, and ΔL_{SAX}, as well as negatively correlated with ΔAR_{Tg}, ΔmW_{RG}, and $\Delta minW_{RG}$. These findings imply that in patients with a more posterior hyoid position, there is greater posterior displacement and deformation of the tongue, increased elevation of the soft palate, and greater reduction of the retroglossal space during airway collapse. Figure 9A–F show that L_{TgU} was positively correlated with ΔL_{LAX}, ΔAR_{Tg}, $\Delta minW_{RP}$, ΔmW_{RG}, and $\Delta minW_{RG}$, as well as negatively correlated with ΔX_{SP}, ΔX_{Tg}, and $\Delta\alpha$. This suggests that in patients with a longer distance between the tongue and the uvula, there is less posterior displacement and deformation of the tongue and soft palate, and less reduction of the retropalatal and retroglossal space during airway obstruction. As shown in Figure 10A–E, the correlation between $minW_{RP}$ and dynamic changes was similar to that of X_{Ho}. This observation indicates that in patients with larger retropalatal space, there is greater posterior displacement and deformation of the tongue, as well as increased reduction of the retroglossal space.

Discussion

In this study, we investigated the collapse process of the upper airway during natural sleep in patients with severe OSA using dynamic MRI. This study identified four distinct types of airway obstruction, including type A, type BI, type BII, and type C based on the obstruction location and motion characteristics. By analyzing the anatomical features of the upper airway and its surrounding tissues, we clarified the tissue movements and morphological changes in each obstruction pattern. Moreover, we evaluated the differences in the anatomical features of patients with different obstruction patterns during normal breathing and explored the correlation between anatomical features and dynamic changes, which shed light on the key anatomical structures that influence the process of airway obstruction.

Patients with type A obstruction have a significantly smaller retropalatal space and a greater distance between the tongue and uvula during normal breathing compared to patients with other obstruction types. In such a case, even a small posterior displacement of the soft palate can result in retropalatal obstruction. The flow rate through the very narrow

Table 2 Anatomical Measurement Results in Patients with Different Obstruction Types A, BI, BII, and C

	Type A (n = 7)	Type BI (n = 9)	Type BII (n = 2)	Type C (n = 5)	P(A-BI)	P(A-BII)	P(A-C)	P(BI- BII)	P(BI-C)	P(BII-C)
Age, years	50.00 ± 11.79	39.22 ± 8.69	46.00 ± 0.00	42.40 ± 6.54	0.114	0.889	0.432	0.145	0.438	0.381
BMI, $kg \cdot m^{-2}$	27.29 ± 5.71	28.57 ± 3.89	24.60 ± 2.26	26.40 ± 1.42	0.252	0.889	0.639	0.218	0.298	0.381
AHI, times/h	54.66 ± 15.02	60.93 ± 17.78	42.10 ± 15.41	56.76 ± 8.39	0.758	0.333	1.000	0.145	0.898	0.190
X_{Ho}, mm	−39.28 ± 2.95	−36.91 ± 3.51	−37.87 ± 0.85	−34.03 ± 3.24	0.252	1.000	**0.010**	1.000	0.112	0.095
Y_{Ho}, mm	5.01 ± 7.33	3.42 ± 5.47	−0.39 ± 10.00	−1.64 ± 8.07	0.470	0.500	0.149	0.727	0.190	1.000
X_{SP}, mm	−21.98 ± 4.39	−22.86 ± 2.36	−19.59 ± 3.87	−23.39 ± 5.76	0.470	0.667	0.755	0.436	0.797	0.571
Y_{SP}, mm	74.39 ± 8.89	70.35 ± 5.97	69.53 ± 20.85	67.83 ± 6.07	0.470	0.889	0.268	1.000	0.364	1.000
L_{SP}, mm	36.18 ± 7.21	38.46 ± 6.63	34.99 ± 5.15	34.37 ± 5.88	0.758	0.889	0.530	0.582	0.438	1.000
α, °	150.29 ± 7.01	143.54 ± 6.61	140.28 ± 13.32	142.52 ± 12.59	0.091	0.333	0.106	1.000	0.364	1.000
β, °	162.84 ± 7.71	165.20 ± 4.57	166.42 ±8.84	166.21 ± 6.15	0.470	0.667	0.530	1.000	0.606	0.857
X_{Tg}, mm	−44.41 ± 5.28	−45.07 ± 3.16	−40.59 ± 0.48	−43.27 ± 4.38	0.536	0.500	0.755	0.145	0.364	0.381
Y_{Tg}, mm	46.39 ± 9.95	46.96 ± 6.43	43.16 ± 18.56	42.35 ± 6.60	0.681	0.889	0.876	1.000	0.240	1.000
L_{LAX}, mm	81.82 ± 8.17	83.23 ± 6.18	81.89 ± 17.16	86.18 ± 3.97	0.470	0.889	0.268	1.000	0.438	1.000
L_{SAX}, mm	48.69 ± 4.24	46.09 ± 3.89	45.87 ± 0.03	47.18 ± 1.98	0.606	0.667	0.639	0.582	0.898	1.000
AR_{Tg}	1.69 ± 0.18	1.82 ± 0.24	1.79 ± 0.37	1.83 ± 0.16	0.536	1.000	0.343	0.909	0.898	1.000
L_{TgU}, mm	33.41 ± 2.82	30.67 ± 1.35	30.22 ± 1.15	29.76 ± 1.49	0.071	0.222	**0.018**	0.582	0.438	0.571
$minW_{RP}$, mm	3.34 ± 1.59	4.15 ± 1.45	4.63 ± 0.97	5.72 ± 1.62	0.351	0.333	**0.048**	1.000	0.112	0.571
mW_{RG}, mm	11.89 ± 2.58	13.73 ± 4.89	10.90 ± 1.93	9.44 ± 2.07	0.758	0.667	0.149	0.436	**0.042**	0.571
$minW_{RG}$, mm	8.20 ± 2.30	9.65 ± 4.30	7.38 ± 2.08	6.48 ± 2.07	0.606	0.889	0.343	0.727	0.240	0.857

Notes: Data are presented as mean ± SD. Bold means significant difference (P<0.05).

Abbreviations: BMI, body mass index; AHI, apnea-hypopnea index; X_{Ho} and Y_{Ho}, the position of the hyoid center in the X-direction and Y-direction; X_{SP} and Y_{SP}, the position of the soft palate center in the X-direction and Y-direction; L_{SP}, the soft palate length; α, the angle between the hard and soft palate; β, the angle between the soft palate and uvula; X_{Tg} and Y_{Tg}, the position of the tongue center in the X-direction and Y-direction; L_{LAX}, the long axis of the tongue; L_{SAX}, the short axis of the tongue; AR_{Tg}, the aspect ratio of the tongue; L_{TgU}, the distance between the tongue center and the tip of the uvula; $minW_{RP}$, the minimum width of the retropalatal space; $minW_{RG}$, the minimum width of the retroglossal space; mW_{RG}, the mean width of the retroglossal space.

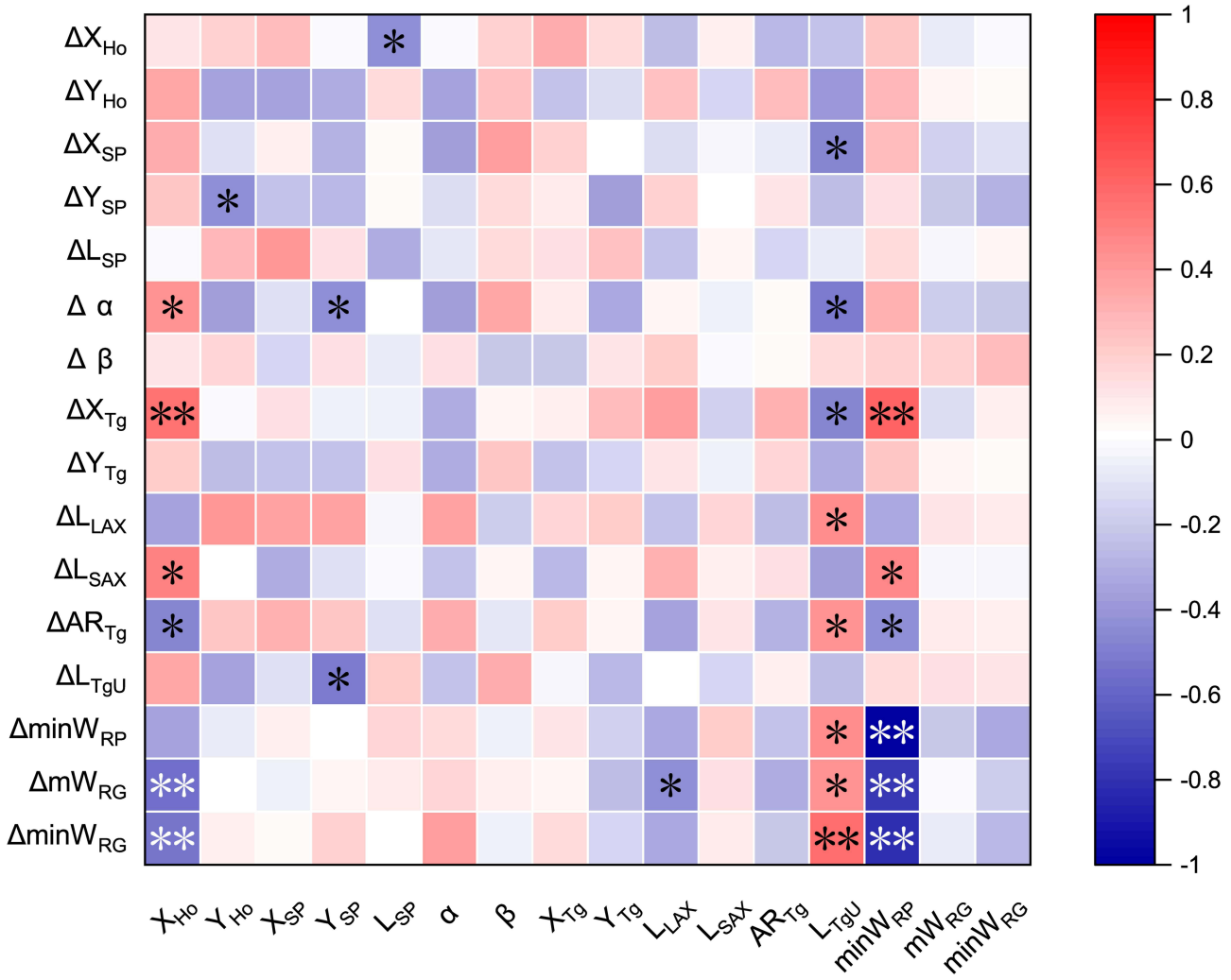

Figure 7 Correlation of the anatomical parameters during normal breathing and the parameter changes during airway obstruction. *P < 0.05, **P < 0.01. R value is represented by color. The horizontal axis shows the anatomical parameters of the upper airway during normal breathing. The vertical axis shows the changes of parameter during airway obstruction.

Abbreviations: X_{Ho} and Y_{Ho}, the position of the hyoid center in the X-direction and Y-direction; X_{SP} and Y_{SP}, the position of the soft palate center in the X-direction and Y-direction; L_{SP}, the length of soft palate; α, the angle between the hard and soft palate; β, the angle between the soft palate and uvula; X_{Tg} and Y_{Tg}, the position of the tongue center in the X-direction and Y-direction; L_{LAX}, the long axis of the tongue; L_{SAX}, the short axis of the tongue; AR_{Tg}, the aspect ratio of the tongue; L_{TgU}, the distance between the tongue center and the tip of uvula; $minW_{RP}$, the minimum width of the retropalatal space; mW_{RG}, the mean width of the retroglossal space; $minW_{RG}$, the minimum width of the retroglossal space; Δ, the change in the parameter.

retropalatal space can be very high, resulting in a large negative pressure there during inspiration, which pulls the tip of the uvula towards the posterior wall of the airway quickly to block the airway without the additional assistance of tongue displacement. When the retropalatal airway is blocked, there is no further change in downstream airway pressure, and thus, the position of the tongue can remain basically unchanged. Therefore, the primary dynamic characteristic of type A obstruction is the upward rotation of the soft palate around the junction of the hard and soft palates.

Type B obstruction refers to a retropalatal obstruction caused by the movement of the soft palate attached to the tongue. During airway obstruction in type BI, the tongue pushes the soft palate backwards and upwards. As the tongue moves back and up, the hyoid moves up, the soft palate rotates upward around the junction between the hard and soft palate, and the soft palate itself becomes more curved. We found two patients with type B obstruction, where the tongue moved backward and downward, more of a retropalatal obstruction due to uvula elongation. In these cases, the hyoid also moves backward and downward and the soft palate rotates downward around the junction between the hard and soft palate while its curvature remains essentially constant. Therefore, we speculate that the underlying mechanism is

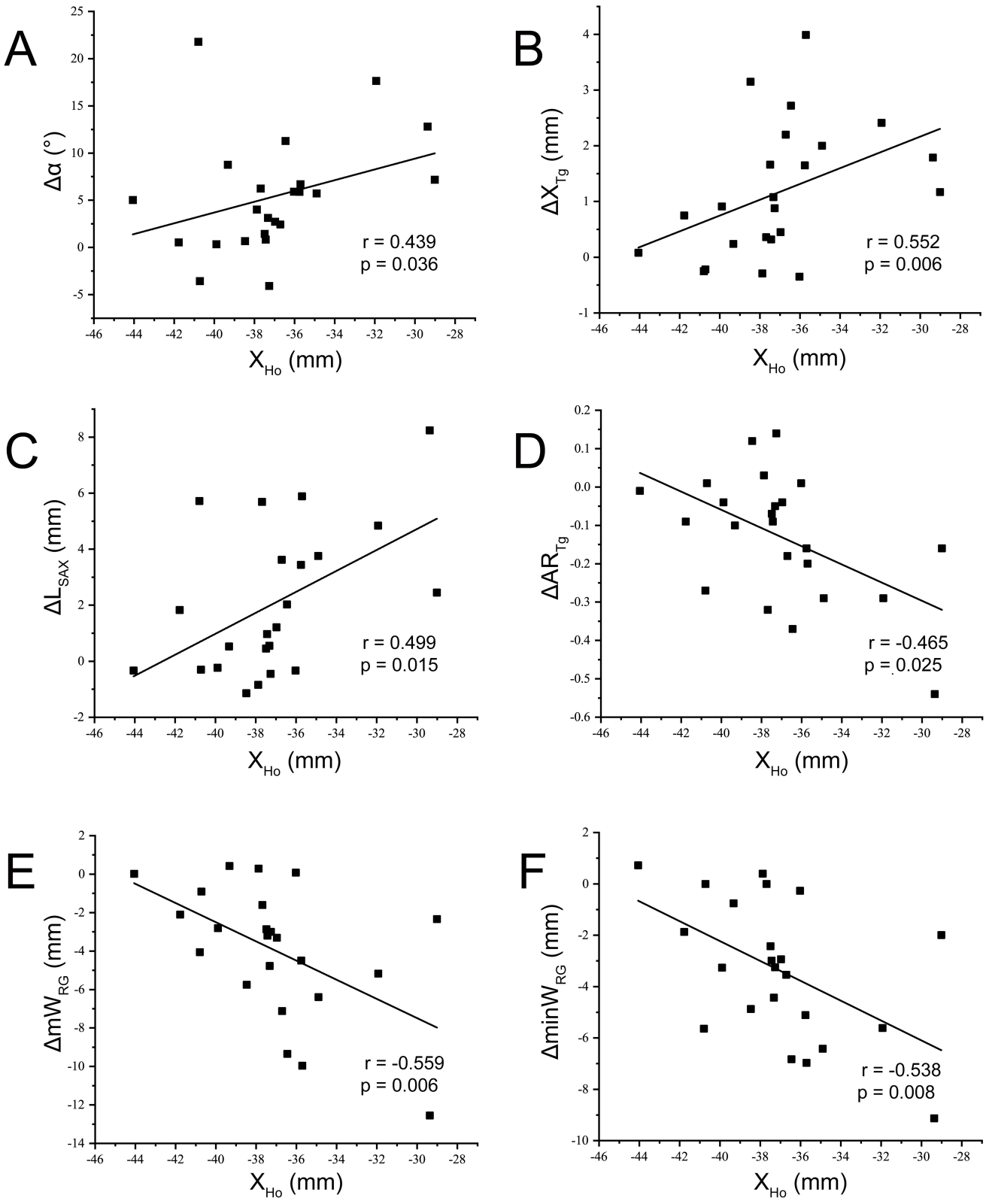

Figure 8 Correlation of the X-direction position of the hyoid, X_{Ho} with (**A**) the difference of the hard palate-soft palate angle, $\Delta\alpha$, (**B**) the displacement of the X-direction position of the tongue, ΔX_{Tg}, (**C**) the difference of the length of the long axis of the tongue, ΔL_{LAX}, (**D**) the difference of the aspect ratio of the tongue, ΔAR_{Tg}, (**E**) the difference of the mean width of the retroglossal space, ΔmW_{RG}, (**F**) the difference of the minimum width of the retroglossal space, $\Delta minW_{RG}$ in all subjects. Solid lines are the fitting results for data from all subjects.

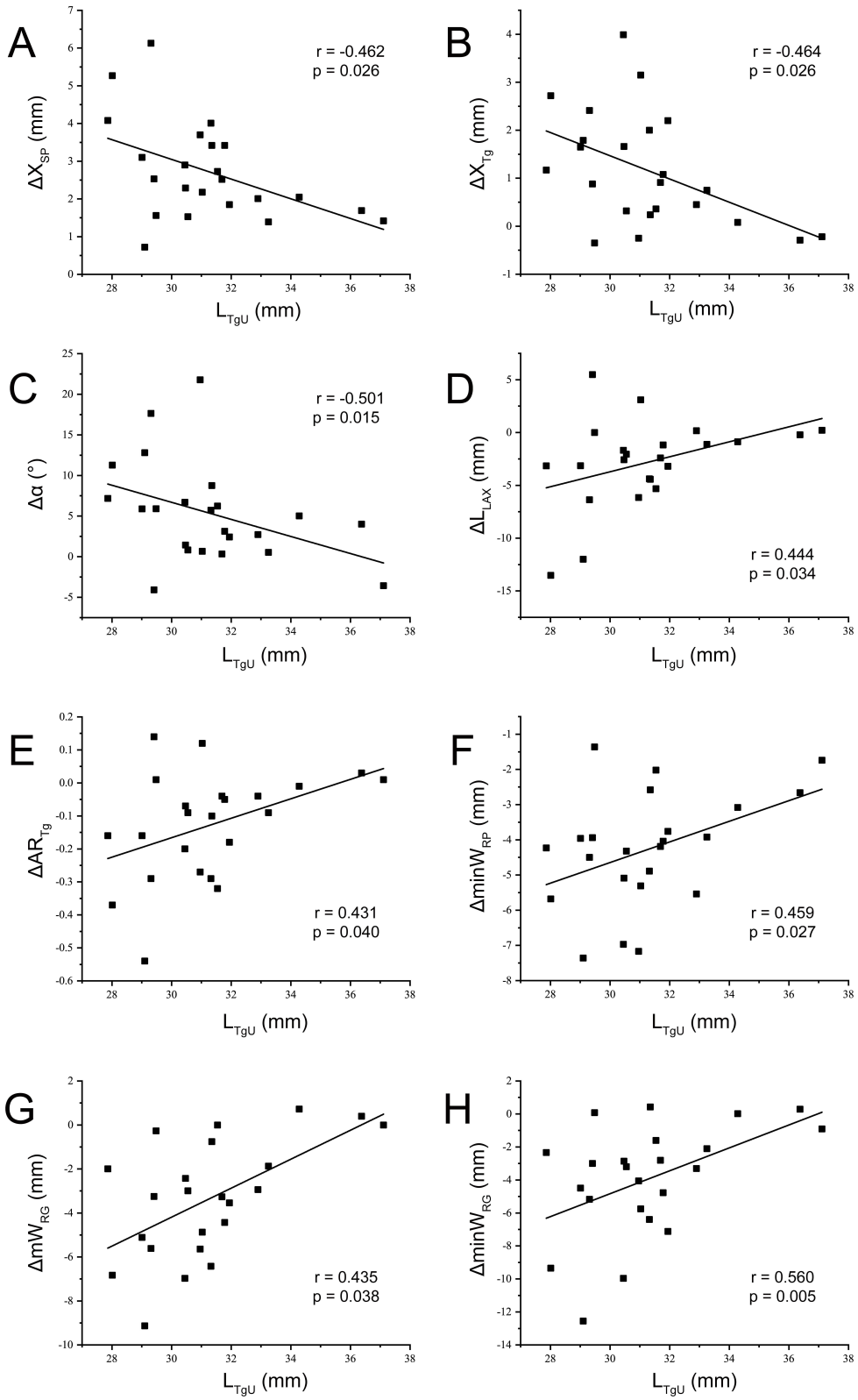

Figure 9 Correlation of the distance between the tongue and uvula, L_{TgU} with (**A**) the displacement of the X-direction position of the soft palate, ΔX_{SP} (**B**) the displacement of the X-direction position of the tongue, ΔX_{Tg}, (**C**) the difference of the hard palate-soft palate angle, $\Delta\alpha$, (**D**) the difference of the length of the long axis of the tongue, ΔL_{SAX}, (**E**) the difference of the aspect ratio of the tongue, ΔAR_{Tg}, (**F**) the difference of the minimum width of the retropalatal space, $\Delta minW_{RP}$ (**G**) the difference of the mean width of the retroglossal space, ΔmW_{RG}, (**H**) the difference of the minimum width of the retroglossal space, $\Delta minW_{RG}$ in all subjects. Solid lines are the fitting results for data from all subjects.

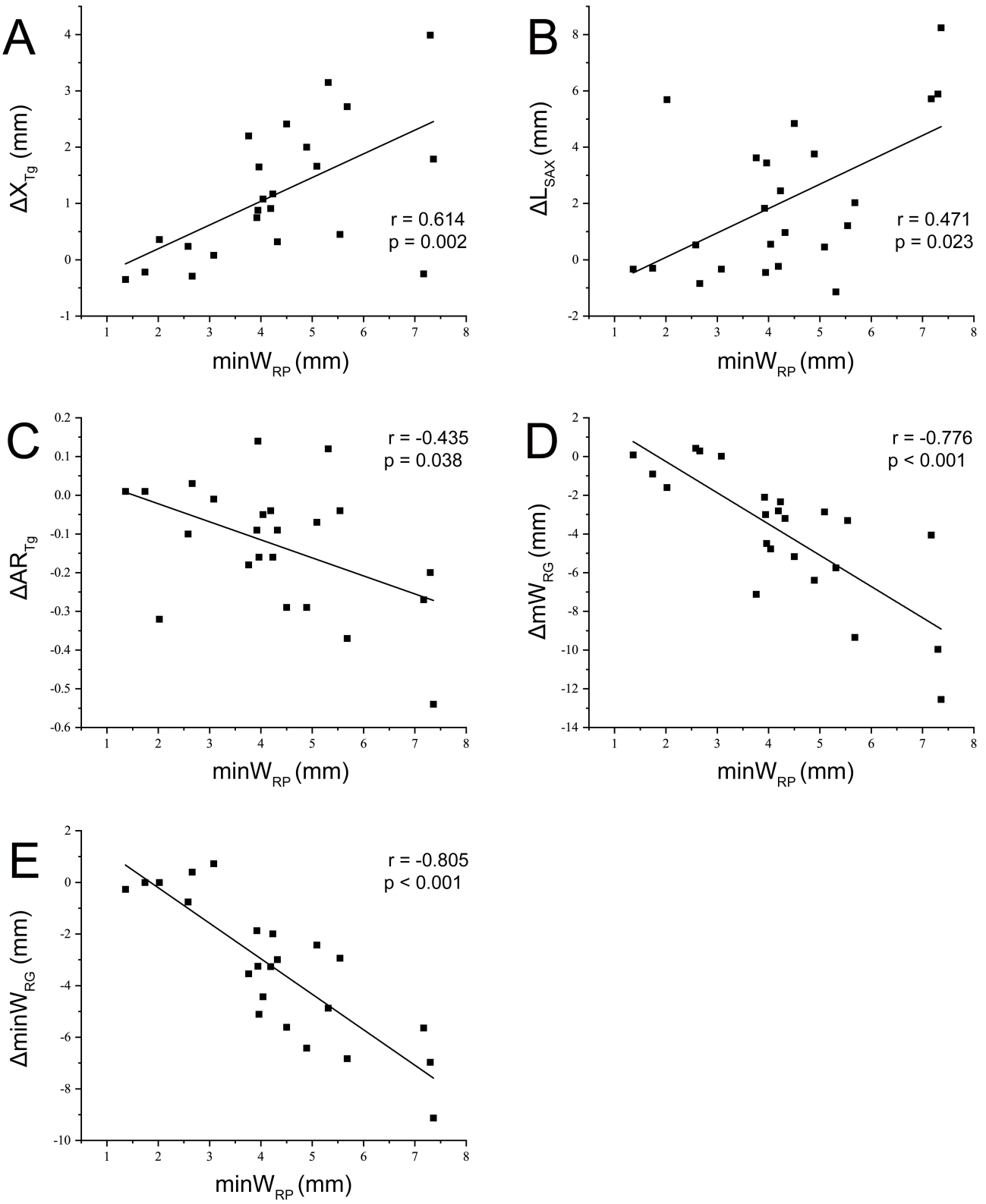

Figure 10 Correlation of the minimum width of the retropalatal space, $minW_{RP}$ with (**A**) the displacement of the X-direction position of the tongue, ΔX_{Tg}, (**B**) the difference of the length of the short axis of the tongue, ΔL_{SAX}, (**C**) the difference of the aspect ratio of the tongue, ΔAR_{Tg}, (**D**) the difference of the mean width of the retroglossal space, ΔmW_{RG}, (**E**) the difference of the minimum width of the retroglossal space, $\Delta minW_{RG}$ in all subjects. Solid lines are the fitting results for data from all subjects.

different from that of type BI obstruction and classify it as type BII obstruction. However, no significant difference is found in the anatomical characteristics of patients with type BI and type BII during normal breathing, and their specific mechanisms need further study.

In patients with type C obstruction, the hyoid is located closer to the posterior wall of the airway during normal breathing than in patients with other types of obstruction, with a larger retropalatal space and a smaller retroglossal space. The larger retropalatal space requires a larger posterior displacement of the tongue to cause retropalatal obstruction, which may result in simultaneous obstruction of the smaller retroglossal space. The movement characteristics of type C airway obstruction are more like an enhanced pattern of type BI. The tongue, soft palate, and hyoid move in same manner as in type BI, but to a greater extent. Importantly, the soft palate rotates more upward, and the soft palate center exhibits a posterior upward displacement due to excessive compression of the tongue.

Our study reveals significant differences in both the anatomical and motor characteristics of the hyoid in different types of airway obstruction. Specifically, from type A to type BI to type C, the hyoid is successively located posterior and inferior during normal breathing, and is successively moved upward with increasing magnitude during airway obstruction. Type BII obstruction differs in that the hyoid is in a similar position to type BI during normal breathing, but moves posteriorly and inferiorly during airway obstruction. These findings suggest that hyoid position may help determine the type of obstruction in OSA patients. Previous imaging studies related OSA have confirmed that the hyoid position in OSA patients differs from that of healthy individuals, and the severity of OSA is related to the size of the downward position of the hyoid.[29,30] This is consistent with our opinion that hyoid plays an important role in the development of OSA. Our study extends upon this and shows that the hyoid location is also a key factor in distinguishing among different types of airway obstruction in OSA patients. Hyoid suspension is often used in clinical practice to treat OSA, and our findings suggest that altering the hyoid position can positively improve obstruction in OSA patients. Previous studies have shown that hyoid suspension significantly reduces the severity of OSA,[31] and is more effective when used in combination with other surgical options.[32,33] Stuck et al reported that hyoid suspension did not improve the upper airway anatomy in OSA patients while awake,[34] but this does not mean that hyoid suspension is ineffective. Our study indicates that the hyoid position is strongly correlated with multiple dynamic characteristics during airway obstruction, including the changes in tongue movement and morphology, the reduction in the retroglossal space, and the changes in the hard-soft palate angle. This suggests that improving hyoid position may not significantly alter the anatomy of the upper airway when awake, but may influence tissues movement during airway obstruction. Therefore, it is recommended that more attention be paid to hyoid-related procedures in future OSA treatment options.

This study also reveals that the minimum width of retropalatal space is associated with multiple dynamic characteristics during airway obstruction. Specifically, the OSA patients with a larger retropalatal space show greater changes in the tongue movement and morphology, as well as greater reductions in airway size during airway obstruction. These findings may help explain the currently low success rate of retropalatal surgery for OSA. Previous studies have shown that patients who do not respond to retropalatal surgery experience more severe airway obstruction.[35] Our study suggests that merely expanding the retropalatal space may not alleviate OSA in some patients and may actually lead to more severe airway obstruction, as previously predicted using the finite element simulation.[36] Therefore, multilevel surgery may be needed to increase the success rate of the surgery in patients with B type obstruction.

Drug-induced sleep endoscopy (DISE) is a widely used clinical technique for the observation of upper airway obstruction in OSA patients. The advantage of DISE is the ability to visually observe the location and degree of airway obstruction in OSA patients. Previous DISE studies have shown that retropalatal obstruction is the dominant site of obstruction.[37,38] However, DISE examines upper airway obstruction under drug-induced sleep, which may differ from natural sleep in terms of upper airway dynamics.[39] DISE also does not provide information on the movement of surrounding tissues such as the tongue and soft palate, which are directly responsible for airway obstruction. Some dynamic studies of the upper airway collapse process have been conducted using CT or MRI. Li et al dynamically observed the process of upper airway collapse under drug-induced sleep through CT, and found that OSA patients had multilevel obstruction, in which the retropalatal airway was the predominant site of obstruction. Complete retropalatal obstruction occurred in 86% of moderate to severe OSA patients.[40] Studies with dynamic MRI for upper airway obstruction indicated that retropalatal obstruction occurred in 98% of OSA patients and retroglossal obstruction in

41% of OSA patients. Most patients with retroglossal obstruction showed concurrent retropalatal obstruction, while only 4% of patients was hypopharynx obstruction.[21] The segmental pattern of upper airway obstruction observed in our study is generally consistent with previous findings in DISE, CT, and MRI studies, highlighting the prevalence of retropalatal obstruction in OSA patients. Our study showed that all patients with severe OSA presented with retropalatal obstruction, and 21.74% of them also had retroglossal obstruction. We should indicate that the four categories we made were purely based on the events of airway obstruction captured in this study. We do not rule out other types of obstruction, such as the obstruction in retroglossal area only or in epiglottis region. However, due to the limited data and the differences in the characteristics of patients participated in different studies, we did not capture these types of obstruction, and therefore, they were not included in the classification of the current study. An important difference from previous studies on airway obstruction is that our study not only classifies the patterns of upper airway obstruction, but also provides insights into the specific movement process and mechanism of each type of obstruction.

There are still some limitations in this study. In order to clearly distinguish the characteristic differences, only Asian male patients with severe OSA are included in this study. Whether the study results are applicable to OSA patients of other races, female OSA patients, or patients with mild to moderate OSA needs further investigation. In addition, this study only examine the process of airway collapse in the mid-sagittal plane of the head and neck, and therefore cannot assess the lateral collapse of the upper airway. The method of using nasal airflow signals to determine whether a OSA patient is asleep can effectively serve the purpose of the current study, but may have limitations for studies that require determination of sleep degree. Due to the technical difficulties in acquiring dynamic MRI during natural sleep, the sample size in this study is relatively small. The 120-second scan is relatively short in duration, likely capturing mainly the light sleep stage, and the four types of obstruction consist of just 112 obstruction events. Larger sample sizes can help identify more distinctive features of different types of obstruction, especially in patients with newly identified type BII obstruction.

Conclusions

This study proposed a novel categorization of upper airway obstruction on the sagittal plane and distinguished four different patterns with varying behavioral characteristics. The motions of the tongue, soft palate and hyoid, as well as associated airway dynamic changes were analyzed in the different patterns of collapse. Moreover, this investigation scrutinized the anatomical features of the upper airway during normal breathing among in patients with different types of obstruction and identified the hyoid position and retropalatal space as the key factors influencing upper airway obstruction.

Data Sharing Statement

The data that support the findings of this study are available from the corresponding author Professor Yaqi Huang upon reasonable request.

Ethics Approval and Consent to Participate

This study was approved by the Ethics Committee of Capital Medical University and we made sure that each participant had signed written informed consent.

Acknowledgments

Special thanks to Wenyue Xiao for her contribution in the drafting of Figure 2. We thank all subjects who participated in this study.

Author Contributions

All authors made a significant contribution to the work reported, whether that is in the conception, study design, execution, acquisition of data, analysis and interpretation, or in all these areas; took part in drafting, revising or critically reviewing the article; gave final approval of the version to be published; have agreed on the journal to which the article has been submitted; and agree to be accountable for all aspects of the work.

Funding

This work was supported by the National Natural Science Foundation of China (Grant Numbers: 34670959, 81171422, 11902209).

Disclosure

The authors report no conflicts of interest in this work.

References

1. Malhotra A, White DP. Obstructive sleep apnoea. *Lancet*. 2002;360(9328):237–245. doi:10.1016/S0140-6736(02)09464-3
2. Gottlieb DJ, Punjabi NM. Diagnosis and management of obstructive sleep apnea: a review. *JAMA*. 2020;323(14):1389–1400. doi:10.1001/jama.2020.3514
3. Ryan CM, Bradley TD. Pathogenesis of obstructive sleep apnea. *J Appl Physiol*. 2005;99(6):2440–2450. doi:10.1152/japplphysiol.00772.2005
4. Schwartz AR, Patil SP, Laffan AM, Polotsky V, Schneider H, Smith PL. Obesity and obstructive sleep apnea: pathogenic mechanisms and therapeutic approaches. *Proc Am Thorac Soc*. 2008;5(2):185–192. doi:10.1513/pats.200708-137MG
5. Evans EC, Sulyman O, Froymovich O. The goals of treating obstructive sleep apnea. *Otolaryngol Clin North Am*. 2020;53(3):319–328. doi:10.1016/j.otc.2020.02.009
6. Caporale M, Palmeri R, Corallo F, et al. Cognitive impairment in obstructive sleep apnea syndrome: a descriptive review. *Sleep Breath*. 2021;25(1):29–40. doi:10.1007/s11325-020-02084-3
7. Moon IJ, Han DH, Kim JW, et al. Sleep magnetic resonance imaging as a new diagnostic method in obstructive sleep apnea syndrome. *Laryngoscope*. 2010;120(12):2546–2554. doi:10.1002/lary.21112
8. Kavcic P, Koren A, Koritnik B, Fajdiga I, Groselj LD. Sleep magnetic resonance imaging with electroencephalogram in obstructive sleep apnea syndrome. *Laryngoscope*. 2015;125(6):1485–1490. doi:10.1002/lary.25085
9. Liu SY, Huon LK, Lo MT, et al. Static craniofacial measurements and dynamic airway collapse patterns associated with severe obstructive sleep apnoea: a sleep MRI study. *Clin Otolaryngol*. 2016;41(6):700–706. doi:10.1111/coa.12598
10. Aurora RN, Casey KR, Kristo D, et al. Practice parameters for the surgical modifications of the upper airway for obstructive sleep apnea in adults. *Sleep*. 2010;33(10):1408–1413. doi:10.1093/sleep/33.10.1408
11. Schwab RJ, Pasirstein M, Pierson R, et al. Identification of upper airway anatomic risk factors for obstructive sleep apnea with volumetric magnetic resonance imaging. *Am J Respir Crit Care Med*. 2003;168(5):522–530. doi:10.1164/rccm.200208-866OC
12. Suratt PM, Dee P, Atkinson RL, Armstrong P, Wilhoit SC. Fluoroscopic and computed tomographic features of the pharyngeal airway in obstructive sleep apnea. *Am Rev Respir Dis*. 1983;127(4):487–492. doi:10.1164/arrd.1983.127.4.487
13. deBerry-Borowiecki B, Kukwa A, Blanks RH. Cephalometric analysis for diagnosis and treatment of obstructive sleep apnea. *Laryngoscope*. 1988;98(2):226–234. doi:10.1288/00005537-198802000-00021
14. Lowe AA, Fleetham JA, Adachi S, Ryan CF. Cephalometric and computed tomographic predictors of obstructive sleep-apnea severity. *Am J Orthod Dentofac Orthop*. 1995;107(6):589–595. doi:10.1016/S0889-5406(95)70101-X
15. Schwab RJ. Upper airway imaging. *Clin Chest Med*. 1998;19(1):33–54. doi:10.1016/S0272-5231(05)70430-5
16. Schwab RJ, Goldberg AN. Upper airway assessment: radiographic and other imaging techniques. *Otolaryngol Clin North Am*. 1998;31(6):931–968. doi:10.1016/S0030-6665(05)70100-6
17. Welch KC, Foster GD, Ritter CT, et al. A novel volumetric magnetic resonance imaging paradigm to study upper airway anatomy. *Sleep*. 2002;25(5):532–542. doi:10.1093/sleep/25.5.530
18. Finkelstein Y, Wolf L, Nachmani A, et al. Velopharyngeal anatomy in patients with obstructive sleep apnea versus normal subjects. *J Oral Maxillofac Surg*. 2014;72(7):1350–1372. doi:10.1016/j.joms.2013.12.006
19. Lin H, Xiong H, Ji C, et al. Upper airway lengthening caused by weight increase in obstructive sleep apnea patients. *Respir Res*. 2020;21(1):272. doi:10.1186/s12931-020-01532-8
20. Suto Y, Matsuo T, Kato T, et al. Evaluation of the pharyngeal airway in patients with sleep-apnea - value of ultrafast MR imaging. *Am J Roentgenol*. 1993;160(2):311–314. doi:10.2214/ajr.160.2.8424340
21. Volner K, Chao S, Camacho M. Dynamic sleep MRI in obstructive sleep apnea: a systematic review and meta-analysis. *Eur Arch Otorhinolaryngol*. 2022;279(2):595–607. doi:10.1007/s00405-021-06942-y
22. Kojima T, Kawakubo M, Nishizaka MK, et al. Assessment by airway ellipticity on cine-MRI to differentiate severe obstructive sleep apnea. *Clin Respir J*. 2018;12(3):878–884. doi:10.1111/crj.12598
23. Feng Y, Keenan BT, Wang S, et al. Dynamic upper airway imaging during wakefulness in obese subjects with and without sleep apnea. *Am J Respir Crit Care Med*. 2018;198(11):1435–1443. doi:10.1164/rccm.201711-2171OC
24. Drummond GB. Comparison of sedation with midazolam and ketamine: effects on airway muscle activity. *Br J Anaesth*. 1996;76(5):663–667. doi:10.1093/bja/76.5.663
25. Eastwood PR, Platt PR, Shepherd K, Maddison K, Hillman DR. Collapsibility of the upper airway at different concentrations of propofol anesthesia. *Anesthesiology*. 2005;103(3):470–477. doi:10.1097/00000542-200509000-00007
26. Ehsan Z, Mahmoud M, Shott SR, Amin RS, Ishman SL. The effects of anesthesia and opioids on the upper airway: a systematic review. *Laryngoscope*. 2016;126(1):270–284. doi:10.1002/lary.25399
27. Wang Y, Mcdonald JP, Liu Y, Pan K, Zhang X, Hu R. Dynamic alterations of the tongue in obstructive sleep apnea-hypopnea syndrome during sleep: analysis using ultrafast MRI. *Genet Mol Res*. 2014;13(2):4552–4563. doi:10.4238/2014.June.17.7
28. Wang YL, Mcdonald JP, Liu YH, Pan KF, Zhang XH, Hu RD. Analysis of the dynamic changes in the soft palate and uvula in obstructive sleep apnea-hypopnea using ultrafast magnetic resonance imaging. *Genet Mol Res*. 2014;13(4):8596–8608. doi:10.4238/2014.January.24.16

29. Jo JH, Park JW, Jang JH, Chung JW. Hyoid bone position as an indicator of severe obstructive sleep apnea. *BMC Pulm Med*. 2022;22(1):349. doi:10.1186/s12890-022-02146-0
30. Genta PR, Schorr F, Eckert DJ, et al. Upper airway collapsibility is associated with obesity and hyoid position. *Sleep*. 2014;37(10):1673–1678. doi:10.5665/sleep.4078
31. Song SA, Wei JM, Buttram J, et al. Hyoid surgery alone for obstructive sleep apnea: a systematic review and meta-analysis: hyoid Surgery for OSA. *Laryngoscope*. 2016;126(7):1702–1708. doi:10.1002/lary.25847
32. Verse T, Baisch A, Maurer JT, Stuck BA, Hörmann K. Multilevel surgery for obstructive sleep apnea: short-term results. *Otolaryngol Head Neck Surg*. 2006;134(4):571–577. doi:10.1016/j.otohns.2005.10.062
33. Baisch A, Maurer JT, Hörmann K. The effect of hyoid suspension in a multilevel surgery concept for obstructive sleep apnea. *Otolaryngol Head Neck Surg*. 2006;134(5):856–861. doi:10.1016/j.otohns.2006.01.015
34. Stuck BA, Neff W, Hormann K, et al. Anatomic changes after hyoid suspension for obstructive sleep apnea: an MRI study. *Otolaryngol Head Neck Surg*. 2005;133(3):397–402. doi:10.1016/j.otohns.2005.06.002
35. Kezirian EJ. Nonresponders to pharyngeal surgery for obstructive sleep apnea: insights from drug-induced sleep endoscopy. *Laryngoscope*. 2011;121(6):1320–1326. doi:10.1002/lary.21749
36. Huang Y, White DP, Malhotra A. The impact of anatomic manipulations on pharyngeal collapse: results from a computational model of the normal human upper airway. *Chest*. 2005;128:1324–1330. doi:10.1378/chest.128.3.1324
37. Zhang P, Ye J, Pan C, et al. Comparison of drug-induced sleep endoscopy and upper airway computed tomography in obstructive sleep apnea patients. *Eur Arch Otorhinolaryngol*. 2014;271(10):2751–2756. doi:10.1007/s00405-014-3051-1
38. Certal VF, Pratas R, Guimarães L, et al. Awake examination versus DISE for surgical decision making in patients with OSA: a systematic review. *Laryngoscope*. 2016;126(3):768–774.39. doi:10.1002/lary.25722
39. Blumen MB, Latournerie V, Bequignon E, Guillere L, Chabolle F. Are the obstruction sites visualized on drug-induced sleep endoscopy reliable? *Sleep Breath*. 2015;19(3):1021–1026. doi:10.1007/s11325-014-1107-5
40. Li HY, Lo YL, Wang CJ, et al. Dynamic drug-induced sleep computed tomography in adults with obstructive sleep apnea. *Sci Rep*. 2016;6:35849. doi:10.1038/srep35849